

Off Ship Measurement of Ship Air Wakes Using Instrumented Unmanned Aerial Vehicles

Murray Snyder^{1,2}

*George Washington University, Washington, DC 20052
 United States Naval Academy, Annapolis, MD 21402*

Anil Kumar³ and Pinhas Ben-Tzvi⁴

George Washington University, Washington, DC 20052

This paper details an innovative method for measuring and investigating off ship air wakes that develop during the operation of naval vessels in common underway wind conditions. Wind currents, both naturally occurring and those resulting from ship motion, can create ship air wakes that make operation of rotary wing aircraft in the vicinity of the ship particularly challenging. Currently extensive underway flight testing is required to determine safe wind over deck launch and recovery envelopes for rotary wing aircraft. This underway flight testing can be difficult to schedule and is very expensive since it involves multiple flights of manned helicopters. Small unmanned TREX 600 radio controlled (RC) helicopters have been equipped with a custom data package that includes an Inertial Measurement Unit (IMU), Global Positioning System (GPS) receiver and transmitter. The instrumented TREX 600 helicopter is flown back and forth through the ship air wake from YP676, which is a dedicated 108 ft long US Naval Academy research vessel, and detects the impact of the associated ship air wake on the 4.3 ft rotor diameter helicopter. IMU and GPS data are transmitted in real time to another data package mounted on the ship. The ship data package also records pilot control inputs to the helicopter. Through the use of a MATLAB script the TREX 600 helicopter position relative to the ship is determined in real time. Received IMU data from the helicopter is also filtered through a trained neural network which removes IMU oscillations due to pilot flight control inputs. Air wake data A_ω is then determined which measures the intensity of the air wake on the TREX 600 helicopter. Comparison of the air wake data A_ω show good correlation to regions of significant air wake intensity predicted by advanced Computational Fluid Dynamics (CFD) simulations.

Nomenclature

A_ω	=	Air Wake Intensity Data
BPNN	=	Back Propagation Neural Network
CFD	=	Computational Fluid Dynamics
GPS	=	Global Positioning System
IMU	=	Inertial Measurement Unit
INS	=	Inertial Navigation System
PWM	=	Pulse Width Modulated
RC	=	Radio Controlled
RF	=	Radio Frequency
β	=	Relative wind angle on horizontal plane

¹ Professor, Mechanical and Aerospace Engineering Department, George Washington University (GWU), 725 23rd Street NW, AIAA Member.

² Research Professor, Aerospace Engineering Department, US Naval Academy, 590 Holloway Road.

³ Graduate Student, Mechanical and Aerospace Engineering Department, GWU, 801 22nd Street NW.

⁴ Associate Professor, Mechanical and Aerospace Engineering Department, GWU, 801 22nd Street NW.

- ω = Raw angular velocity measurement data from Gyroscope
- ω_f = Low pass filtered angular velocity data
- ω_r = Neural Network compensated angular velocity data
- ω_s = Standard deviation filtered angular velocity data
- ω_s' = Neural Network predicted standard deviation filtered angular velocity data

I. Introduction

LAUNCH and recovery of rotary wing aircraft from naval vessels can be very challenging and potentially hazardous. Ship motion combined with the turbulence that is created as the wind flows over the ship's superstructure can result in rapidly changing flow conditions for rotary wing aircraft. Additionally, dynamic interface effects between the vessel air wake and the rotor wake are also problematic.

To ensure aircraft and vessel safety, launch and recovery envelopes are prescribed for specific aircraft types on different ship classes (Fig. 1).¹ Permissible launch and recovery envelopes are often restrictive because of limited flight envelope expansion. Flight testing required to expand the envelopes is frequently difficult to schedule, expensive and potentially hazardous. Currently, the launch and recovery wind limits and air operation envelopes are primarily determined via the subjective analysis of test pilots (e.g. excessive flight control inputs are required to safely land on the flight deck), using a time consuming and potentially risky iterative flight test build-up approach. The time and risk of flight testing could be reduced through the complementary use of computational tools to predict test conditions and extrapolate test results, thereby reducing the number of actual flight test points required. However, current computational methods are insufficiently validated for ships with a complex superstructure, such as a destroyer or cruiser.²⁻⁹ Validated computational air wake predictions can also be used for ship design and operational safety analysis.

Much effort has been expended to validate CFD predictions of ship air wakes above the flight decks of naval vessels, primarily through the use of ultrasonic anemometers. Within the limits of variable atmospheric boundary layers, ocean wave effects and ship motion the CFD codes are considered reasonably accurate for the region above the flight deck.^{8,10,11} However, significantly less validation data is available for the CFD prediction of off ship air wakes. This paper presents a new and innovative method to indirectly measure ship air wake effects away from the flight deck region where placement of ultrasonic anemometers is currently not feasible.

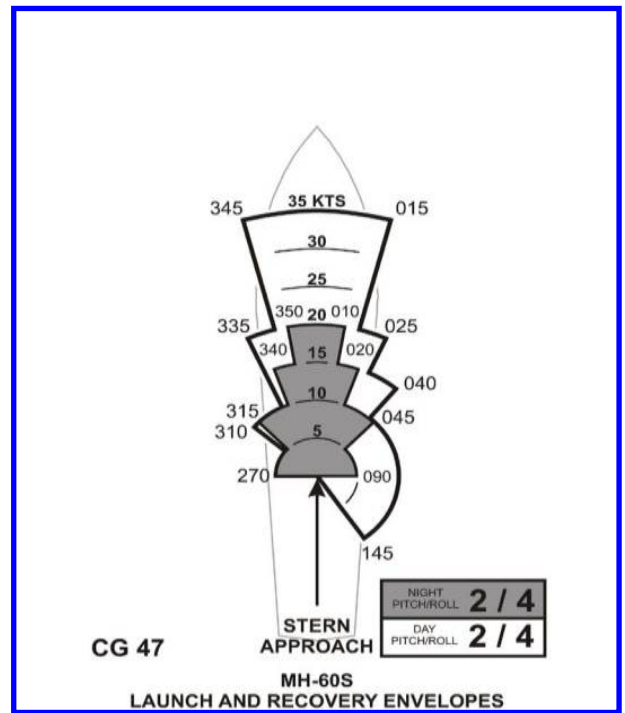


Figure 1. Launch and recovery envelopes, showing allowable relative wind over deck, for MH-60S helicopters on USS Ticonderoga (CG 47) class cruiser (Ref. 1).

II. Off Ship Air Wake Measurement System

The system discussed herein makes use of a small RC helicopter with rotor diameter of 1.3 m (4.3 ft) to estimate ship air wakes. The instrumentation system is used to estimate turbulence patterns in the air wake aft of the Naval Academy's YP676 training vessel (Fig. 1a). The system uses an IMU as its basic sensor and correlates the helicopter's vibration with ship air wakes. The system is a technological successor to instrumentation system presented in our prior work^{12,13} and is composed of two identical instrumentation boards, where one is located on the helicopter and acts as transmitter while the other is located on the naval vessel and acts as a receiver. Figure 1b shows the RC helicopter retrofitted with the instrumentation board and flotation. The YP676 vessel was equipped with a bow mounted anemometer sensor array, GPS and electronic compass to help the vessel's Craftmaster to generate the desired relative wind condition. The instrumented helicopter was then maneuvered in a back and forth trajectory in the region aft of the underway vessel. The light weight RC helicopter, weighing approximately 5 kg (11 lbs), is significantly influenced by the ship air wakes and hence the onboard IMU senses the vibrations induced by air wake interaction. IMU and GPS data from the helicopter is wirelessly transmitted to the workstation located in the flight deck of the YP676 vessel, where this data is combined with GPS and compass data from the boat to map the helicopter's vibrational data with its location trajectory relative to the ship.



Figure 1a. Modified YP676 naval training vessel with flight deck (left); b). RC helicopter with retrofitted instrumentation board and flotation system (right).

Ship air wake is an example of a turbulent air flow, which is characterized by a high wind velocity gradient. Such velocity gradient exerts non-uniform loading on rotary wings and makes the helicopter rotate about the direction given the curl of local wind field in addition to linear drifting.¹⁴ Such rotation is hence an important characteristic of ship air wake and can be easily measured with the help of a Gyroscope present within the IMU package.¹⁵ Through extensive experimentation it was inferred that it is not only the angular velocity that characterizes air wake, but also variations in the angular velocity. Thus, the product of magnitude of angular velocity and standard deviation of angular velocity was taken as a measure for air wake intensity. Since the RC helicopter is controlled by using a swash plate mechanism, any maneuver will result in tilting of the helicopter. Therefore, the Gyroscope signals contains some component that is due to helicopter's maneuvers resulting from pilot inputs. In order to use Gyroscope signals for air wake estimation it is important to remove the components arising from pilot inputs. A Futaba 8-channel radio frequency (RF) receiver (identical to the RF receiver on helicopter) was used with the system's receiver to capture pilot inputs in the form of five pulse width modulated (PWM) control signals transmitted by the pilot's radio transmitter. The system was designed to acquire data at a refresh rate of 45 Hz. Data from sensors with low refresh rate like GPS was linearly interpolated to match with other faster sensors. Figure 2 shows a schematic diagram of the current instrumentation system.

This paper presents the use of Back Propagation Neural Networks (BPNN) as a filter to remove pilot input components from measured gyro signals. The angular velocity measured by the gyroscope, being a vector quantity, can be treated as a vector sum of rotations caused by pilot control inputs and ship air wake. Thus by training the BPNN to predict angular velocity from pilot input data, the ship air wake component in the gyroscope can be estimated by simple vector subtraction. As the helicopter maneuvers in the air wake of the underway vessel, the vibrations are captured, corrected for pilot inputs and then combined with the helicopter's location to obtain relative ship air wake information.

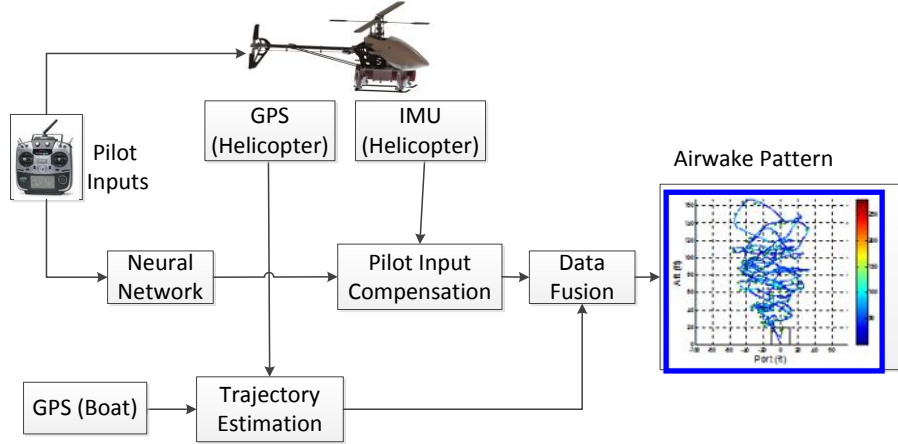


Figure 2. Schematic of instrumentation system.

III. Neural Network for Pilot Input Compensation

Artificial Neural Networks or simply Neural Networks are one of the most commonly used machine learning techniques used in robotics. Neural networks can be seen as a directed acyclic graph with computational units (called as neurons or perceptron's) as its nodes¹⁶⁻¹⁸. Each neuron is a multiple input single output system where the output is computed by applying an activation function on weighted sum of input data.

$$y = f(\mathbf{w}^T \mathbf{x} + b) \quad (1)$$

Here y is the output of the neuron, \mathbf{x} is the input vector, \mathbf{w} is the weight vector, b is bias and f is the activation function. A neural network is defined by the structure (topology) of the network and the type of activation function of the involved neurons. Thus training of a neural network involves estimation of optimal weights and biases. BPNN is a multilayer feed-forward network that uses an error back propagation algorithm¹⁸⁻²⁰ for training. In the current application, BPNNs are trained to predict response of helicopter's gyroscope to pilot inputs in an air wake free environment. The predictions from these networks are then used for pilot input compensation during actual field-testing of the system in the Chesapeake Bay area.

A. Data preprocessing for BPNN training

As the helicopter's motion is controlled by swash plate mechanism, the attitude of the helicopter depends on vector thrusting by tilt of the swash plate (cyclic control). The angular velocity of the helicopter is thus the result of the change in cyclic control from the pilot and this change can be quantized by the rate of change in the servo input signals.¹⁵ Thus all the pilot input channels are modeled as a linear function of time ($y = m \cdot t + b$) in a fixed window of N samples using least square methods. Here y is the PWM signal in one of the pilot input channels in the given window of time and t is the corresponding time index. The line parameters m and b are estimated using the least square method as follows:

$$m = \frac{N \sum_{i=1}^N t_i y_i - \sum_{i=1}^N t_i \cdot \sum_{i=1}^N y_i}{N \sum_{i=1}^N t_i^2 - (\sum_{i=1}^N t_i)^2}, \quad b = \frac{\sum_{i=1}^N t_i^2 \cdot \sum_{i=1}^N y_i - \sum_{i=1}^N t_i \cdot \sum_{i=1}^N t_i y_i}{N \sum_{i=1}^N t_i^2 - (\sum_{i=1}^N t_i)^2}. \quad (2)$$

In order to account for the imperfections in modeling of pilot input patterns, deviation from the linear fit was also considered as a pilot input parameter and was estimated as follows:

$$e = \sum_{i=1}^N |s_i - (m t_i + b)|. \quad (3)$$

Here s_i is the actual PWM signal input as obtained from the RC receiver. Thus all the three parameters $\{m, b, e\}$ were estimated for each of the five pilot input channels to obtain a 15 dimensional input feature space for neural network training.

The high-speed rotation of the rotor wings introduces large quantities of high frequency noise into the IMU reading and the frequency of noise is much higher than the frequencies of oscillations resulting from ship air wakes or pilot inputs. In the current system this high frequency noise is filtered with the help of a Gaussian low pass filter. If ω is the three dimensional raw gyroscope data then the corresponding low-pass filtered data (ω_f) is obtained by the application of Gaussian low pass filter with cut-off frequency of 1.05 Hz. The cut-off frequency was selected on the basis of spectrum analysis of the pilot input signals and air wake data.

As the air wake intensity is characterized by product of magnitude of angular velocity and standard deviation of angular velocity, a total of four channels of gyroscope data were predicted by the BPNN. Three of them were Cartesian components of gyroscope data with low pass Gaussian filter and the fourth channel was the local standard deviation of the magnitude of the gyroscope data. In total four neural networks were trained to predict each of the four gyroscope data channels and had one dimensional output space.

B. Neural network topology

Neural networks have three components: input layer, hidden layer and output layer. The number of nodes in the input and output layers of neural network are determined by the dimensionality of the input and the output data. Thus each of the four neural networks had 15 nodes in the input layer and one node in output layer. To accommodate sufficient room for nonlinearity in the helicopter's response to pilot inputs, two hidden layers were selected for each of the networks. The number of nodes in the hidden layers was selected using a "trial and error" method, and then analyzing network performance with actual data. The numbers of nodes in the two hidden layers of each of the four neural networks were as follows: {10,7}, {9,8}, {10,8} and {10,8}. With the commonly used Levenberg–Marquardt algorithm²¹⁻²² for error back propagation training, the hidden layers and the output layer used "tansig" and "purelin" functions respectively as their activation functions.²³ The neural networks were trained with 10-fold cross validation²⁴ to prevent over-training and loss of generalization.

C. BPNN performance in modeling helicopter response to pilot inputs

To model the helicopter's response to pilot inputs, the training data for the neural network was collected from indoor flights conducted in a large aircraft hangar at Davison Army Airfield. The hangar provided a closed environment, free from any kind of air disturbance and thus helped in measuring vibrational response of helicopter to pilot inputs. Six indoor training flights each with duration of around 10 minutes (~27,000 samples) were conducted using three different helicopters. This paper presents results from one of the three helicopters (TREX ESP 600). During the neural network training process 25% of the total data (~55,000 samples from two flights) was used for training the network and the remaining 75% was used for testing and assessing the network performance.

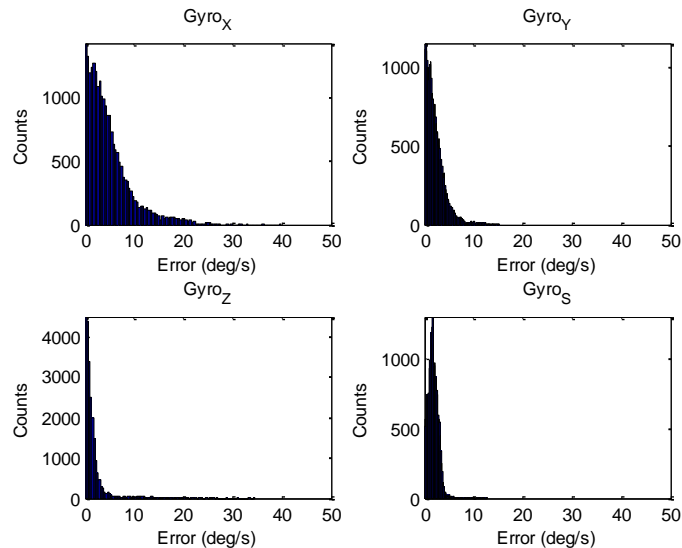


Figure 3. Predication error distribution of neural networks.

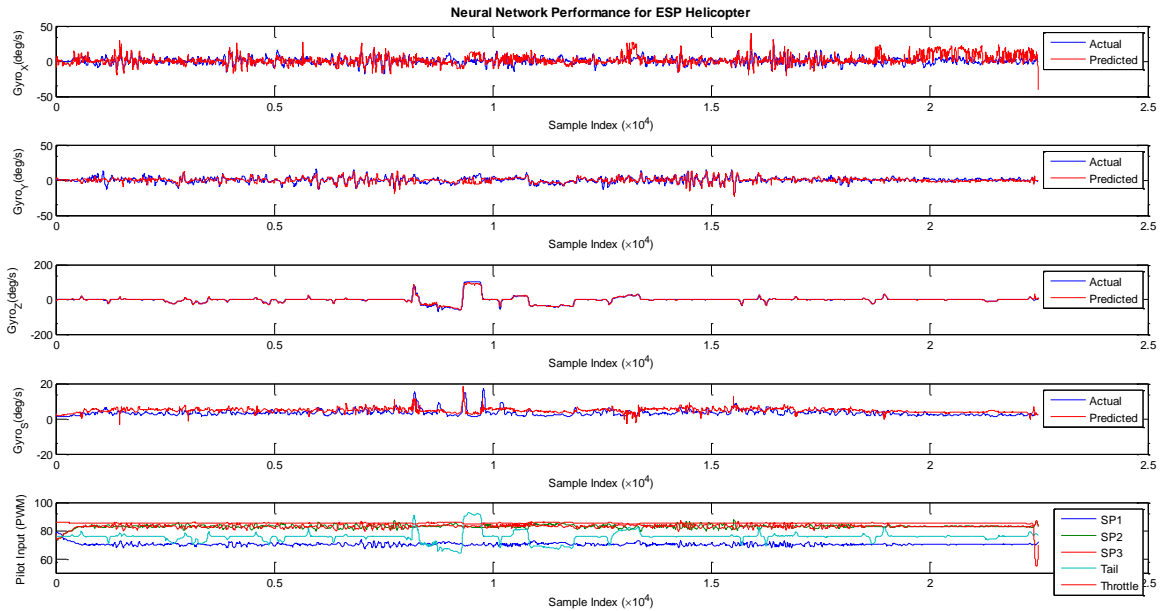


Figure 4. Prediction results of neural networks based on indoor flight data.

Figure 3 shows histogram plots of the prediction error of all the four neural networks. The skewed shape of the histograms towards zero error corroborates the capability of the trained neural networks in estimating pilot input components in helicopter's gyroscope response. The actual prediction results along with pilot input signals are shown in Fig. 4 where actual measurement in blue color is overlaid on BPNN prediction in red. Again, high degree of prediction accuracy is visible in these results as the plots overlap with each other very well. In this figure, $Gyro_x$, $Gyro_y$, $Gyro_z$ and $Gyro_s$ refer to Cartesian components of angular velocity (along X , Y and Z axes) and the local standard deviation in angular velocity, respectively.

IV. Air wake pattern estimation

As mentioned earlier, this paper models ship air wake with both angular velocity and standard deviation of angular velocity. Thus there is a need for pilot input compensation in both angular velocity and its standard deviation. If $\{\omega_x, \omega_y, \omega_z\}$ is the low-pass filtered gyroscope data (ω_f) from the helicopter in Cartesian coordinate system and $\{\omega_x', \omega_y', \omega_z'\}$ is the corresponding pilot input components estimated from three Neural Networks, then the compensated magnitude of angular velocity (ω_r) can be estimated as follows:

$$\omega_r = \sqrt{(\omega_x - \omega_x')^2 + (\omega_y - \omega_y')^2 + (\omega_z - \omega_z')^2} \quad (4)$$

Since the components arising from the helicopter's own motion were removed from the filtered measurements, the resultant angular velocity was a measure of external disturbance (ship air wake). It was also observed that both the ship air wakes and helicopters' motion cause variations in angular velocity measurements. Thus, standard deviation was used as a good measure of air wake intensity and hence requires pilot input compensation as well. The local standard deviation (ω_s) of the magnitude of the gyroscope data (ω) in a window of length N samples (~ 1 sec data) is calculated as follows:

$$\omega_s(i) = \sqrt{\frac{\sum_{d=-N/2}^{+N/2} \left(\omega(i+d) - \frac{1}{N} \sum_{x=-N/2}^{+N/2} \omega(i+x) \right)^2}{N}} \quad (5)$$

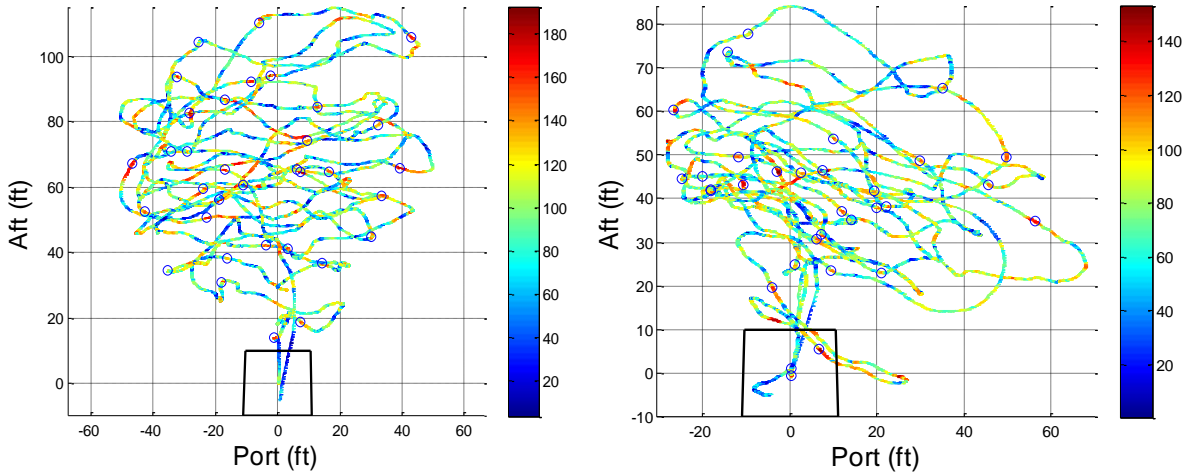


Figure 5. Estimated ship air wake pattern for β angles 0° and 15° .

where $i \in I [1, L]$ and L is total number of samples in ω . The standard deviation of the angular velocity as calculated in Eq. (5) is compensated for the pilot input component by subtracting the standard deviation estimated from for the fourth neural network. Eq. (6) shows the actual air wake intensity obtained as the product of the compensated angular velocity and the compensated local standard deviation

$$A_\omega(i) = (\omega_s(i) - \omega_s'(i)) \times \omega_r(i); \quad i \in I [1, L] \quad (6)$$

where ω_s' is the local standard deviation of the gyro data predicted from the Neural Network. The ship air wake intensity being a function of relative position with respect to naval vessels makes better sense when represented in relation to the relative trajectory. The trajectory of the helicopter was obtained in the boat's frame of reference by using the GPS locations of the YP676 and the helicopter along with the YP676's heading direction as obtained from the onboard digital compass.

V. Results, Conclusions and Future Work

The current system was tested underway in the Chesapeake Bay to experimentally determine the ship air wake patterns generated by YP676. During test flights, the wind relative to the boat was maintained at approximately 15 knots of relative wind for two different β angles of 0° and 15° , where β is measured from bow of the ship in clockwise direction using the anemometer array mounted on the bow of YP676. The helicopter's altitude was maintained at the YP676's upper deck level throughout the test flight to ensure repeatability in the results.

Figure 5 shows air wake intensity distribution as estimated by Eqn. (6), overlaid on the helicopter's trajectory in the YP676's frame of reference. In these plots the color represent air wake intensity patterns for beta angles 0° and 15° , respectively. The high air wake intensity zones are concentrated along the centerline in air wake distribution for beta angle 0° and tilted to the right of the central line in the air wake distribution for beta angle 15° . These results are show reasonable correlation to the predicted air wakes for $\beta = 0$ and 15° .¹⁵

The knowledge of rotational disturbances from ship air wake is important for safe operation of helicopters on naval vessels, but is not sufficient on its own. A significant component of the ship air wake causes lateral drift in the helicopter, which needs to be taken care of. Currently, the authors are working to add an Inertial Navigation System (INS) to the instrumentation system to estimate the absolute linear velocity of the helicopter.

Future work in this area will also include the following:

(1) Use of more robust machine leaning techniques such as Linear Bayesian Regression to estimate the pilot component that contributes to the helicopter's translational motion and compensate for the same. This combination of translational and rotational disturbances will certainly give better description of ship air wake patterns using this instrumentation system.

(2) The instrumented RC helicopter will be flown through a "known" air wake in a large hangar to calibrate system response. The known air wake will be generated with industrial fans blowing air over a backward facing step and will be measured with ultrasonic anemometers placed in multiple locations downwind from the fans and backward facing step.

(3) Development of a method for directly measuring off ship air wakes using an RC helicopter carrying two ultrasonic anemometers that would use RF to transmit real time anemometer data as the helicopter visits various test points away from the ship. The anemometer data would then be corrected for helicopter motion and attitude. A notional schematic of this system is shown in Fig. 6 below.



Figure 6. Proposed TREX 600 helicopter with anemometers for direct measurement of air wakes.

References

- ¹“Helicopter operating procedures for air-capable ships NATOPS manual,” NAVAIR 00-08T-122, 2003.
- ²Guillot, M.J. and Walker, M.A., “Unsteady analysis of the air wake over the LPD-16,” *AIAA 2000-4125: 18th Applied Aerodynamics Conference*, Denver, Colorado, 2000.
- ³Guillot, M.J., “Computational simulation of the air wake over a naval transport vessel,” *AIAA Journal*, Vol. 40, No. 10, 2002, pp. 2130-2133.
- ⁴Lee, D., Horn, J.F., Sezer-Uzol, N., and Long, L.N., “Simulation of pilot control activity during helicopter shipboard operations,” *AIAA 2003-5306: Atmospheric Flight Mechanics Conference and Exhibit*, Austin, Texas, 2003.
- ⁵Carico, D., “Rotorcraft shipboard flight test analytic options,” *Proceedings 2004 Institute of Electrical and Electronics Engineers (IEEE) Aerospace Conference*, Vol. 5, Big Sky, Montana, 2004.
- ⁶Lee, D., Sezer-Uzol, N., Horn, J.F., and Long, L.N., “Simulation of helicopter ship-board launch and recovery with time-accurate air wakes,” *Journal of Aircraft*, Vol. 42, No. 2, 2005, pp. 448-461.
- ⁷Geder, J., Ramamurti, R. and Sandberg, W.C., “Ship air wake correlation analysis for the San Antonio Class Transport dock Vessel,” *Naval Research Laboratory paper MRL/MR/6410-09-9127*, May 2008.
- ⁸Polisky, S., Imber, R., Czerwec, R., & Ghee, T., “A Computational and Experimental Determination of the Air Flow Around the Landing Deck of a US Navy Destroyer (DDG): Part II,” *AIAA-2007-4484: 37th AIAA Fluid Dynamics Conference and Exhibit*, Miami, Florida, 2007.
- ⁹Roper, D. M., Owen, I., Padfield, G.D. and Hodje, S.J., “Integrating CFD and pilot simulations to quantify ship-helicopter operating limits,” *Aeronautical Journal*, Vol. 110, No. 1109, 2006, pp. 419-428.
- ¹⁰Luznik, L., Brownell, C.J. and Snyder, M.R., “Influence of the Atmospheric Surface Layer on a Turbulent Flow Downstream of a Ship Superstructure,” *Journal of Atmospheric and Oceanic Technology*, 30-1, pp. 1803-1819 (2013).
- ¹¹Snyder, M.R., Kang, H.S., Brownell, C.J. and Burks, J.S., “Validation of Ship Air Wake Simulations and Investigation of Ship Air Wake Impact on Rotary Wing Aircraft,” *Naval Engineers Journal*, 125-1, pp. 49-50 (2013).
- ¹²Snyder, M.R., Kumar, A., Ben-Tzvi, P. and Kang, H.S., “Validation of Computational Ship Air Wakes for a Naval Research Vessel,” *AIAA Paper 2013-0959: AIAA 51st Aerospace Sciences Meeting*, Grapevine, Texas, Jan. 7-10, 2013.
- ¹³Kumar, A., Ben-Tzvi, P., Snyder, M.R., Saab, W., “Instrumentation System for Ship Airwake Measurement”, *Proceedings of the 2013 IEEE International Symposium on Robotic and Sensors Environments (ROSE 2013)*, Washington, DC, Oct. 21-23, 2013

- ¹⁴U.S. Department of Transportation, FAA *Helicopter Flying Handbook*: Online:
http://www.faa.gov/regulations_policies/handbooks_manuals/aviation/helicopter_flying_handbook/
- ¹⁵Metzger, J.D., Snyder, M.R., Burks, J.S. and Kang, H.S., "Measurement of Ship Air Wake Impact on a Remotely Piloted Aerial Vehicle," *American Helicopter Society 68th Annual Forum*, Fort Worth, Texas, May 2012.
- ¹⁶Rojas, R., "Neural Networks - A Systematic Introduction", Springer-Verlag, Berlin, New-York, 1996, pp 151-184.
- ¹⁷Haykin, S., "Neural Networks: A Comprehensive Foundation", Prentice-Hall, Englewood Cliffs, NJ, 1999.
- ¹⁸Simpson, P.K., "Artificial Neural Systems" Pergmon Press Elmsford, New York, 1989.
- ¹⁹Karmin, E., "A simple procedure for pruning backpropagation trained neural networks", *IEEE Transactions on Neural Networks*, 1(2), 1990, pp. 239-242.
- ²⁰Widrow, B., and S.D. Sterns, "Adaptive Signal Processing," New York, Prentice-Hall, 1985.
- ²¹Marquardt D.W., "An algorithm for least-squares estimation of nonlinear parameters," *Journal of the Society for Industrial and Applied Mathematics*, 11(2):431-441, 1963.
- ²²Levenberg K., "A Method for the Solution of Certain Non-Linear Problems in Least Squares". *The Quarterly of Applied Mathematics*, Vol. 2, 1944 pp.164-168.
- ²³Beale M. H., Hagan M.T. and Demuth H. B., Neural Network Toolbox, *MATLAB User's Guide*, Online:
http://www.mathworks.com/help/pdf_doc/nnet/nnet_ug.pdf
- ²⁴Kohavi, R., "A study of cross-validation and bootstrap for accuracy estimation and model selection". *Proceedings of the 14th International Joint Conference on Artificial Intelligence*, 1995, 2(12): pp. 1137-1143.